An evidence-based 3D reconstruction of *Asteroxylon mackiei* the most complex plant preserved from the Rhynie chert

Authors

Alexander J. Hetherington[1,2,*], Siobhán L. Bridson[1], Anna Lee Jones[1,3,4], Hagen Hass[5], Hans Kerp[5], Liam Dolan[1,6,*]

Affiliations

[1]Department of Plant Sciences, University of Oxford, South Parks Road, Oxford, OX1 3RB, UK.

[2]Current address: Institute of Molecular Plant Sciences, School of Biological Sciences, University of Edinburgh, Max Born Crescent, Edinburgh, EH9 3BF, UK.

[3]Department of Plant Sciences, University of Cambridge, Downing Street, Cambridge, CB2 3EA, UK.

[4]Current address: Oxford Long-term Ecology Laboratory, Department of Zoology, University of Oxford, Oxford, OX1 3PS, UK.

[5]Research Group for Palaeobotany, Institute for Geology and Palaeontology, Westfälische Wilhelms-Universität Münster, Heisenbergstrasse 2, 48149 Münster, Germany.

[6]Current address: Gregor Mendel Institute of Molecular Plant Biology GmbH, Dr. Bohr-Gasse 3, 1030 Vienna, Austria.

*Correspondence to sandy.hetherington@ed.ac.uk and liam.dolan@gmi.oeaw.ac.at

Abstract

The 407-million-year-old Rhynie chert preserves the earliest terrestrial ecosystem and informs our understanding of early life on land. However, our knowledge of the 3D structure, and development of these plants is still rudimentary. Here we used digital 3D reconstruction techniques to produce the first complete reconstruction of the lycopsid *Asteroxylon mackiei*, the most complex plant in the Rhynie chert. The reconstruction reveals the organisation of the three distinct axes types – leafy shoot axes, root-bearing axes and rooting axes – in the body plan. Combining this reconstruction with developmental data from fossilised meristems, we demonstrate that the *A. mackiei* rooting axis – a transitional lycophyte organ between the rootless ancestral state and true roots – developed from root-bearing axes by anisotomous dichotomy. Our discovery demonstrates how this unique organ developed, and highlights the value of evidence-based reconstructions for understanding the development and evolution of the first complex plants on Earth.

Introduction

The Silurian-Devonian terrestrial revolution saw the evolution of vascular plants with complex bodies comprising distinct roots, root-bearing organs, shoots and leaves from morphologically simpler ancestors characterised by networks of undifferentiated axes (Bateman et al., 1998; Gensel and Edwards, 2001; Kenrick and Crane, 1997; Stewart and Rothwell, 1993; Xue et al., 2018). The 407-million-year-old Rhynie chert fossil site provides a unique insight into the structure of plants during this key time in plant evolution. The Rhynie chert preserves an entire Early Devonian hot spring ecosystem, where plants, animals, fungi and microbes are preserved *in situ* (Edwards et al., 2018; Garwood et al., 2020; Rice et al., 2002; Strullu-Derrien et al., 2019; Wellman, 2018). The exceptional preservation has been crucial for our understanding of early land plant evolution because it is the earliest time point in the fossil record where cellular details of rhizoid-based rooting systems, germinating spores and fossilised meristems are preserved (Edwards, 2004; Hetherington and Dolan, 2018a, 2018b; Kerp, 2018; Lyon, 1957; Taylor et al., 2005). Most of the detailed cellular information about these organisms comes from sectioned material. While the cellular detail that can be observed in these sections allows high resolution reconstruction of tissue systems, the three-dimensional relationship between the cells, tissue and organs is obscured. This makes generating accurate reconstructions of body plans difficult (Edwards, 2004; Kidston and Lang, 1921). Furthermore, reconstructions that have been published are based on combining material from thin sections from multiple individuals (Kidston and Lang, 1921). These sampling problems mean that key features of the body plans of these organisms are missing in reconstructions. This is particularly problematic for larger, more complex species in the Rhynie chert, such as the lycopsid *Asteroxylon mackiei* (Bhutta, 1969; Edwards, 2004; Edwards et al., 2018; Hetherington and Dolan, 2018a; Kerp, 2018; Kerp et al., 2013; Kidston and Lang, 1921, 1920).

A. mackiei has been reconstructed as a plant that is approximately 30 cm high (Bhutta, 1969; Edwards, 2004), with highly branched shoot and rooting systems (Chaloner and MacDonald, 1980; Kerp, 2018; Kerp et al., 2013; Kidston and Lang, 1921, 1920). It holds an important phylogenetic position for understanding root and leaf evolution in lycophytes because it is a member of the earliest diverging lineage of the lycopsids, the Drepanophycales (Kenrick and Crane, 1997), and both the rooting axes and leaves of *A. mackiei* developed some but not all defining characteristics of roots and leaves in more derived species (Bower, 1908; Hetherington and Dolan, 2018a; Kenrick, 2002; Kidston and Lang, 1920). However, the precise number of distinct axes types and their interconnection is still unclear (Bhutta, 1969; Kidston and Lang, 1921, 1920). Without a complete understanding of the habit of *A. mackiei* it is not possible to compare its structure with living

lycopsids or other Drepanophycalean lycopsids found in Devonian compression fossils. The Drepanophycalean lycopsids are the earliest group of land plants in the fossil record with complex body plans comprising distinct rooting axes, root-bearing organs and leafy shoots (Gensel et al., 2001; Gensel and Edwards, 2001; Hueber, 1992; Kenrick and Crane, 1997; Lang and Cookson, 1935; Matsunaga and Tomescu, 2017, 2016; Stewart and Rothwell, 1993). Their evolution, radiation and spread across all continents contributed to the transformation of the terrestrial environment through their impact on soil formation and stabilisation, surface hydrology and silicate weathering (Algeo and Scheckler, 1998; Gibling and Davies, 2012; Matsunaga and Tomescu, 2016; Xue et al., 2016). Given the recognition of the importance of the Drepanophycalean lycopsids in the evolution of complex body plans and changes to global nutrient and hydrological cycles, we generated a reconstruction of the 3D structure of *A. mackiei* based entirely on serial sections from complete specimens fossilised *in situ*.

Here we report the 3D reconstruction of *A. mackiei* based on both morphology and anatomy of two different plants. This reconstruction allowed us to define the 3D organisation of the three axes types of the *A. mackiei* body and to describe how the rooting system developed.

Results

To discover the structure and infer the development of the lycopsid *A. mackiei*, we produced a series of 31 consecutive thick sections through a block of Rhynie chert (Edwards et al., 2018; Garwood et al., 2020; Rice et al., 2002; Strullu-Derrien et al., 2019; Wellman, 2018) that preserved a branched network of connected *A. mackiei* axes *in situ* (Figure S1, S2). Using images of these thick sections, we digitally reconstructed the *A. mackiei* plant in a volume of 4.8 cm in length, 3.5 cm in width and 2.8 cm in height (Figure 1A, B, Movie S1), which to our knowledge, represents the largest evidence-based reconstruction for any Rhynie chert plant to date. We distinguished three distinct axes types in a single individual plant that we designate; leafy shoot axes, root-bearing axes and rooting axes.

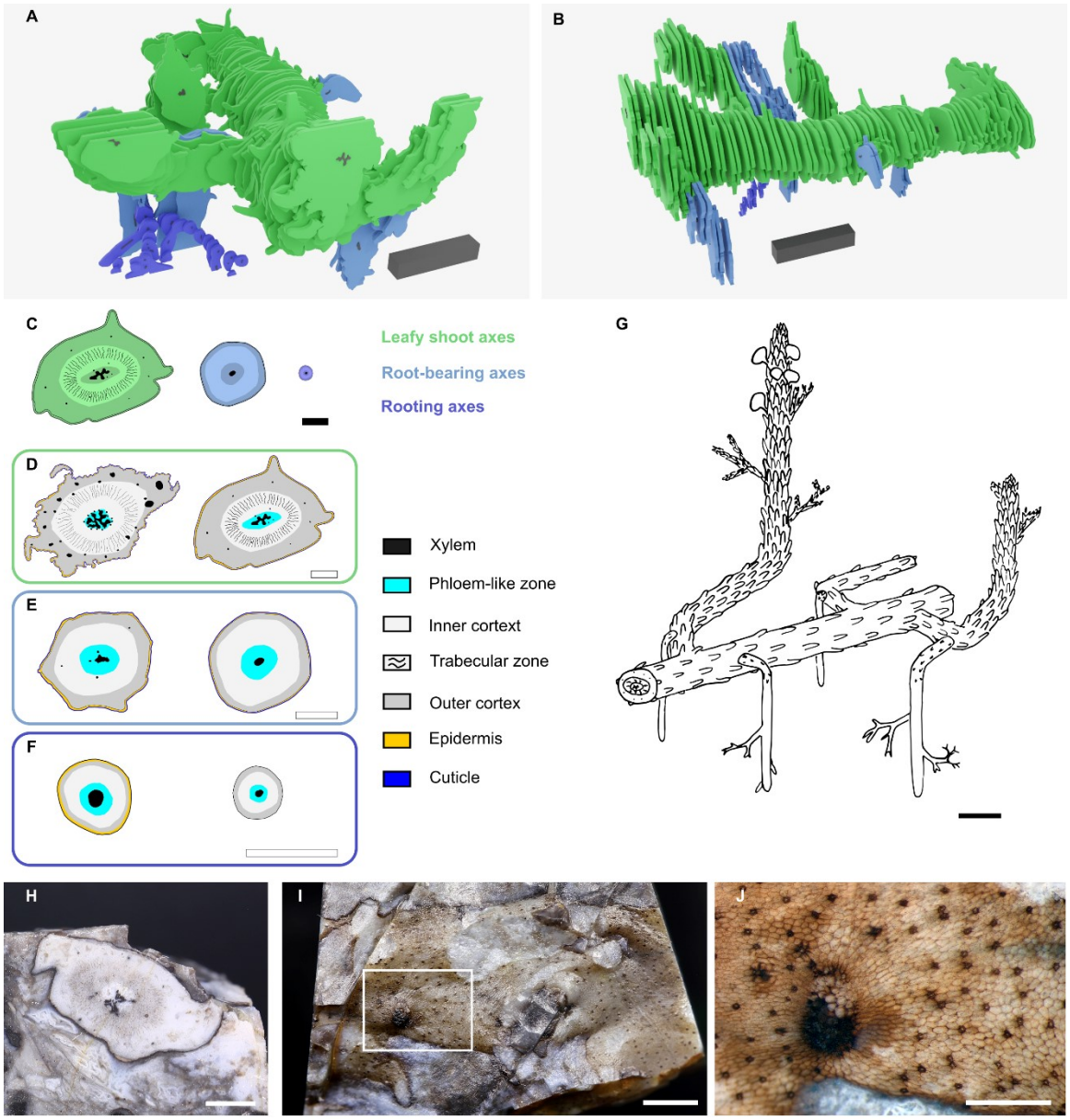

Figure 1. The body plan of *Asteroxylon mackiei* was composed of three distinct axes, leafy shoot axes, root-bearing axes and rooting axes. A, B, 3D reconstruction of *A. mackiei* based on a series of 31 thick sections. C, Representative examples of transverse sections through the three main axis types colour coded to match their colours in the 3D reconstruction (A, B), leafy shoot axes in green, root-bearing axes in blue and rooting axes in purple. D-F, Line drawings of representatives of each of the three main axes types illustrating their anatomy. Examples of two representative leafy shoots (D), root-bearing axes (E) and rooting axes (F). G, An artist's impression of *A. mackiei*. H-J, Example of a plagiotropic leafy shoot exposed on the surface of a block of chert Pb 2020_01. H, End on view of the block of chert with *A. mackiei* leafy shoot axis cut in transverse section. I, Same block as in (H) showing the surface of the axis with brown cuticle and sparse covering of leaves. J, Higher magnification image of white box in (I) showing a single leaf base and abundant stomata. Line drawings of *A. mackiei* axes based on specimen accession codes: GLAHM Kid. 2479 and Pb 4181 (D), Bhutta Collection RCA 13 and RCA 113 (E), GLAHM Kid 2471 and GLAHM Kid 2477 (F). 3D scale bar 1 x 0.1 x 0.1 cm (A, B). Scale bars, 1 cm (G), 2 mm (C-F, H, I), 1 mm (J).

Leafy shoot axes

The majority of the axes in our reconstruction were leafy shoots (Figure 1A, B, Movie S1). Leafy shoot axes developed leaves, abundant stomata and a characteristic internal anatomy including a stellate xylem, many leaf traces and trabecular zone as reported for *A. mackiei* (Bhutta, 1969; Kerp, 2018; Kerp et al., 2013; Kidston and Lang, 1921, 1920; Lyon, 1964) (Figure 1C, D). The presence of a geopetally infilled void in the sections allowed us to determine the orientation of axes relative to the gravitational vector; the main axis present in each of the thick sections was plagiotropic (Figure S1). Four leafy shoot axes with similar anatomy attached to the main axis at anisotomous branch points (Gola, 2014; Imaichi, 2008; Øllgaard, 1979; Yin and Meicenheimer, 2017); an anisotomous branch point is a description of morphology and means that the diameters of the two axes connected at a branch point are different. The diameter of the main plagiotropic leafy shoot was ca. 1 cm and the thinner leafy shoots attached at branch points were ca. 0.6 cm. Some of the thinner leafy shoots were orientated closer to the vertical, indicating orthotropic growth orientation (Figure 1A, B). Although our reconstruction did not include connections between these orthotropic axes and previously described fertile axes, it is likely that some of these orthotropic leafy shoot axes were connected to fertile axes (Bhutta, 1969; Kerp et al., 2013; Lyon, 1964) (Figure 1G). The most noticeable differences between the plagiotropic leafy shoots described here and orthotropic shoots described previously (Bhutta, 1969; Kerp et al., 2013; Kidston and Lang, 1921, 1920; Lyon, 1964), are that the xylem was less lobed and there were fewer leaf traces in the plagiotropic leafy shoot axes than in the orthotropic leafy shoot axes (Figure 1D). Fewer leaf traces in plagiotropic regions is consistent with a lower leaf density on these axes than in orthotropic axes, a feature demonstrated in detail by the discovery of an isolated plagiotropic leafy shoot with sparse covering of leaves preserved on the exterior of a block of chert (Figure H-J). We conclude that *A. mackiei* developed plagiotropic and orthotropic leafy shoot axes with similar anatomy.

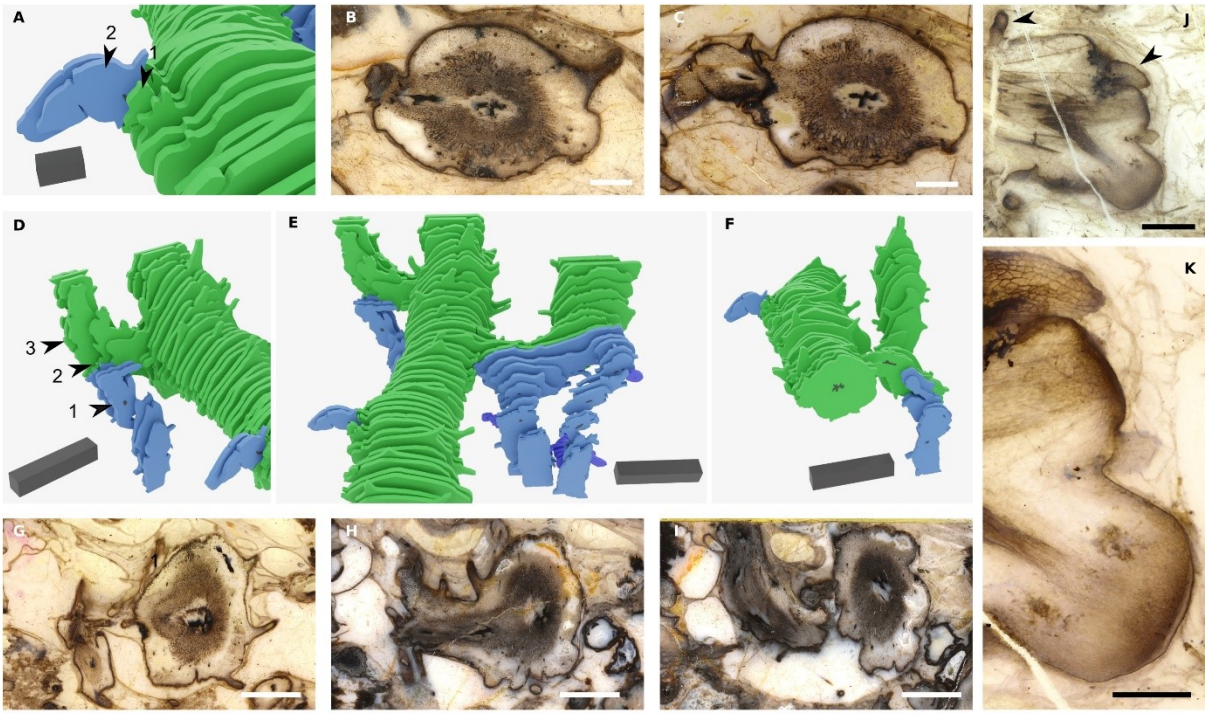

Figure 2. Root-bearing axes attached to leafy shoots at anisotomous branch points. Images showing the attachment of root-bearing axes shown in blue to leafy shoots shown in green based on our 3D reconstruction (A, D-F) and the thick sections used to create the reconstruction (B, C, G-I). A, A root-bearing axis shown in blue attached to the side of the larger plagiotropic leafy shoot axis shown in green. B, The thick section represented by arrow 1 in (A) showing a transverse section through the leafy shoot at the point of branching. The black xylem trace of the rooting axis is located to the left of the cross shaped xylem at the centre of the leafy shoot axis. C, Thick section represented by arrow 2 in (A) showing the free root-bearing axis with small rounded xylem trace compared to the larger cross shaped xylem in the leafy shoot. D-F, Examples based on the reconstruction of *A. mackiei* of root-bearing axes attached to first order leafy shoots close to their attachment with the main leafy shoot. In each case the root-bearing axes are smaller in diameter than the leafy shoots they are attached to and all root-bearing axes are aligned with the gravity vector. G-I, Examples of thick sections showing the anisotomous branch point with attachment of a root-bearing axis and leafy shoot, the position of each thick section is illustrated on the reconstruction in (D), with arrow 1 (G), 2 (H) and 3 (I). J, A bifurcating root-bearing axis with two apices attached to a larger leafy axis (leaves on large axis highlighted with arrowheads). K, Higher magnification image of (J), showing the continuous cuticle covering the two apices and small leaf attached to the lower flank of the upper apex. 3D scale bar 1 x 0.1 x 0.1 cm (D-F), 2 x 1 x 1 mm (A). Scale bars, 5 mm (G-I), 2 mm (B, C,) 1 mm (J), 500 µm (K). Specimen accession codes: Pb 4178 (B), Pb 4177 (C), Pb 4164 (G), Pb 4163 (H), Pb 4162 (I), Pb 2020_02 (J, K).

Root-bearing axes

Root-bearing axes of *A. mackiei* were attached to leafy shoot axes at anisotomous branch points, where the thinner daughter axis developed as a root-bearing axis and the thicker daughter axis developed as a leafy shoot axis (Figure 1, 2). Diameters of root-bearing axes were ca. 0.35 cm compared to leafy shoots axes typically over 0.6 cm. In one of the five

examples (Figure 2A-C) the root-bearing axis was attached directly to the main leafy shoot axis. In the four other examples (Figure 2D-I), root-bearing axes were attached to side branches of the main leafy shoot. These branches were termed first order leafy shoots because they were separated from the main shoot by a single branching event. Root-bearing axes attached to first order leafy shoot axes close to where the latter attached to the main shoot. The branch arrangement where two adjacent anisotomous branches originate close to each other is termed k-branching (Chomicki et al., 2017; Edwards, 1994; Gensel et al., 2001; Gensel and Berry, 2001; Gerrienne, 1988; Matsunaga and Tomescu, 2017, 2016). The root-bearing axes of the Drepanophycalean lycopsid *Sengelia radicans* (Matsunaga and Tomescu, 2017, 2016) are attached to leafy shoot axes at k-branch points. In both *A. mackiei* and *S. radicans,* root-bearing axes developed an epidermis and cuticle with occasional stomata and scale leaves. In the root-bearing axes of *A. mackiei* where anatomy could be investigated the xylem strand was elliptical, not lobed as in leafy shoot axes, and there were few or no leaf traces, which distinguishes them from leafy shoots in which leaf traces were abundant (Figure 1E). Root-bearing axes were aligned with the gravity vector, indicating strong positive gravitropic growth (Figure 1A, B, 2). These differences in anatomy and morphology between root-bearing axes and leafy shoots demonstrate that root-bearing axes were a distinct axis type and not merely a transitional zone between two axis types as previously suggested (Bhutta, 1969; Kidston and Lang, 1921, 1920). The apex of a root-bearing axis had not been described previously. We searched for apices on axes with the characters of root-bearing axes and discovered an isolated bifurcating axis with two apices (Figure 2J, K). The apices were assigned to *A. mackiei* because of the presence of leaves on the parent axis (Figure 2 J, arrowheads) and a small leaf on the flank of the upper apex (Figure 2 J, K), *A. mackiei* is the only Rhynie chert plant with leaves. Both apices were covered by an unbroken cuticle, and a single small leaf was present on the upper apex, which together demonstrate that these are apices of root-bearing axes and not apices of rooting axes that lack leaves and cuticles (Hetherington and Dolan, 2018a), or leafy shoots where the apex is covered by a large number of leaves (Edwards, 2004; Hueber, 1992; Kerp, 2018; Kerp et al., 2013). These apices were found in a single thin section that was not part of a set of serial sections and therefore it was not possible to reconstruct the apex in 3D. The root-bearing axes described here are similar to the axes described as either root-bearing axes (Matsunaga and Tomescu, 2017, 2016) or rhizomes (Rayner, 1984; Schweitzer, 1980; Schweitzer and Giesen, 1980; Xu et al., 2013) in other members of the Drepanophycales. The occurrence of these root-bearing axes in *A. mackiei* and multiple other species highlights the conservation of body plans among members of the Drepanophycales.

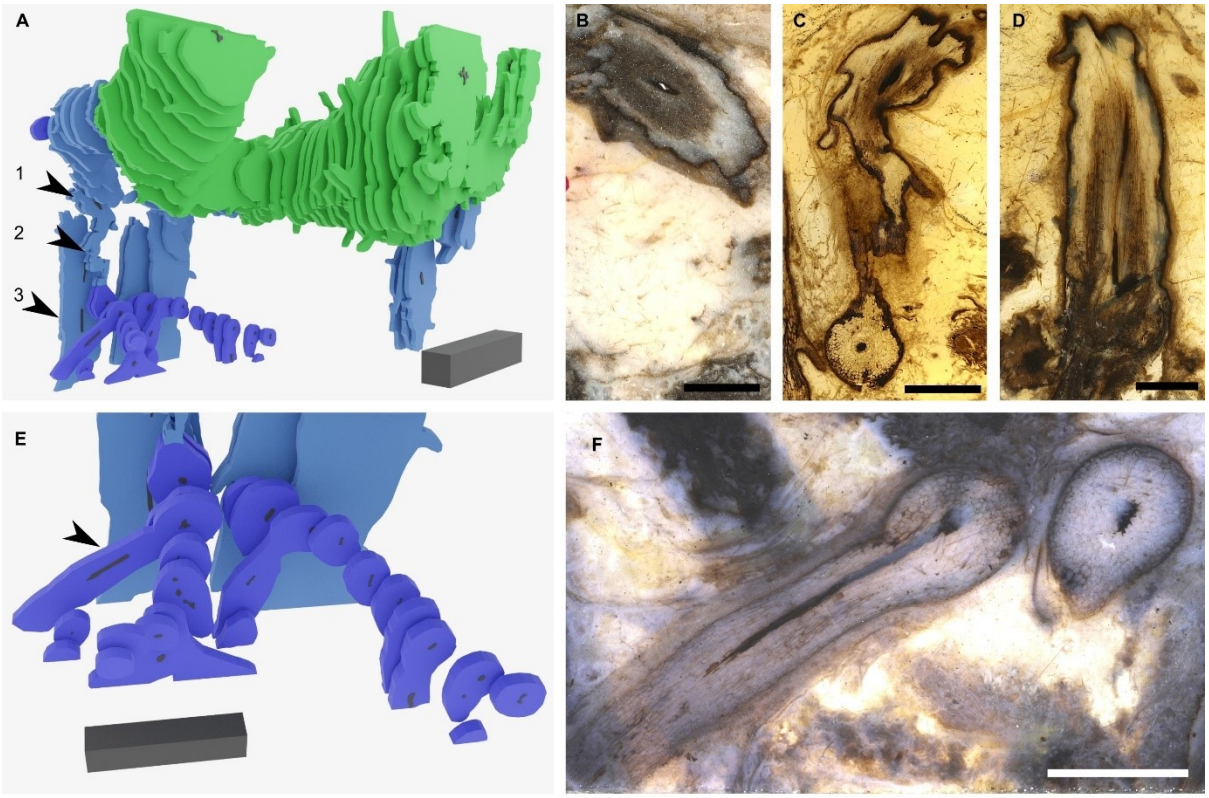

Figure 3. Rooting axes attached to root-bearing axes at anisotomous branch points. A, Connection between a rooting axis in purple and root-bearing axis shown in blue based on the 3D reconstruction. B-D, Three thick sections showing successive stages of the same root-bearing axis preserving the attachment of the rooting axis at an anisotomous branch point. The positions of the three thick sections in the reconstruction (a) are shown with the three numbered arrowheads 1 (B), 2 (C) and 3 (D). E, F, Rooting axes branched profusely, through at least four orders of branching. F, Example branched rooting axis (marked by arrowhead in E). 3D scale bar 1 x 0.1 x 0.1 cm (A), 5 x 1 x 1 mm (E). Scale bars, 2 mm (B, C, D, F). Specimen accession codes: Pb 4174 (B, F), Pb 4175 (C), Pb 4177 (D).

Rooting axes

A. mackiei rooting axes are similar to roots of extant lycopsids. However, they are designated rooting axes because they lack root hairs and their meristems lack a root cap and are consequently interpreted as transitional to the roots of extant plants (Hetherington and Dolan, 2019, 2018a). These rooting axes include rhizomes (Bhutta, 1969), small root-like rhizomes (Kidston and Lang, 1921, 1920) and rooting axes (Hetherington and Dolan, 2019, 2018a) of *A. mackiei* from previous descriptions of plant fragments. Rooting axes were always less than 2 mm in diameter and frequently less than 1 mm and were highly branched (Bhutta, 1969; Hetherington and Dolan, 2018a; Kidston and Lang, 1921, 1920). Leaves, leaf traces, stomata and cuticles were never found on rooting axes, even when the epidermis was well preserved (Kidston and Lang, 1920). The epidermis was frequently missing

suggesting it was lost in older axes and the outer cortex was often limited to one or two cell layers (Figure 1F) (Kidston and Lang, 1920). We found a single well preserved highly branched rooting axis in our reconstruction (Figure 3A-F). This rooting axis was attached to a root-bearing axis at an anisotomous branch point (Figure 3C). There was a circular xylem strand at the centre of the rooting axis. The diameter of the rooting axis where it attached to the root-bearing axis was ca. 2 mm but decreased in size distally at successive branch points. Leaves, leaf traces, stomata and cuticles were never observed on the rooting axis. The rooting axis was weakly gravitropic in contrast to the strong gravitropic growth observed in root-bearing axes (Figure 3A, E). The profuse branching of the rooting axis is evident with over four orders of branching preserved in less than 1 cm in our reconstruction (Figure 3E). We found no evidence that other axis types developed from the rooting axis. The morphological and anatomical boundary between the root-bearing axis and rooting axis was clear (Figure 3C); it involved the change from strong gravitropic growth to weak gravitropic growth, and the absence of scale leaves, stomata and a well-marked cuticle all found on root-bearing axes but absent on rooting axes. This suggests the boundary between the two axes types is defined at the point of branching and not in a continuum along a single axis. The rooting axis and its attachment to root-bearing axes described here corresponds to the axes termed, roots (Matsunaga and Tomescu, 2017, 2016; Schweitzer, 1980; Schweitzer and Giesen, 1980), root-like axes (Gensel et al., 2001; Rayner, 1984) and rootlets (Xu et al., 2013) in other members of the Drepanophycales. This suggests that the body plan of *A. mackiei* was similar to other members of the Drepanophycales.

Our new reconstruction from serial thick sections through an individual *A. mackiei* plant demonstrates that the *A. mackiei* body plan consisted of three distinct axes types – leafy shoot axes, root-bearing axes and rooting axes – each with characteristic anatomy and morphology.

Dichotomous origin of rooting axes

The rooting axes of *A. mackiei* hold a key position for interpreting the origin of roots in lycopsids because they were transitional between the ancestral rootless state and the derived state characterised by true roots with caps as found in extant lycopsids (Hetherington and Dolan, 2019, 2018a). Our new reconstruction enables us to interpret these rooting axes in light of the overall body plan of *A. mackiei*, and in comparison to the rooting axes called roots (Matsunaga and Tomescu, 2017, 2016; Schweitzer, 1980; Schweitzer and Giesen, 1980), root-like axes (Gensel et al., 2001; Rayner, 1984) and rootlets (Xu et al., 2013) in other members of the Drepanophycales. The reconstruction

283 demonstrates further similarities between the rooting axes of *A. mackiei* and the roots
284 (Matsunaga and Tomescu, 2017, 2016; Schweitzer, 1980; Schweitzer and Giesen, 1980),
285 root-like axes (Gensel et al., 2001; Rayner, 1984) and rootlets (Xu et al., 2013) in other
286 Drepanophycales, including attachment to root-bearing axes, weak gravitropic growth and
287 profuse dichotomous branching.

288 These findings suggest that the rooting system of *A. mackiei* was representative of the
289 Drepanophycales and that inferences made with the exceptional preservation of *A. mackiei*
290 can inform about other members of the Drepanophycales for which most plants are
291 preserved only as compressions. Our new reconstruction indicates that rooting axes
292 connected to root-bearing axes at anisotomous branch points. Based on development of
293 extant lycopsids (Bierhorst, 1971; Fujinami et al., 2020; Gola, 2014; Guttenberg, 1966;
294 Harrison et al., 2007; Hetherington and Dolan, 2017; Imaichi, 2008; Imaichi and Kato, 1989;
295 Ogura, 1972; Øllgaard, 1979; Spencer et al., 2020; Yi and Kato, 2001; Yin and
296 Meicenheimer, 2017) there are two modes of branching that could produce anisotomous
297 branch point morphology, endogenous branching or dichotomous branching. Endogenous
298 branching is the mode of branching where the meristem of the new axis develops from the
299 internal tissues of the parent axis and breaks through the parent tissue to emerge, a mode of
300 development typical of the initiation of roots of extant lycopsid species (Bierhorst, 1971;
301 Bruchmann, 1874; Fujinami et al., 2020; Guttenberg, 1966; Hetherington and Dolan, 2017;
302 Imaichi, 2008; Imaichi and Kato, 1989; Ogura, 1972; Øllgaard, 1979; Wigglesworth, 1907; Yi
303 and Kato, 2001). Dichotomous branching is the mode of branching where the parent
304 meristem splits in two to produce two daughter axes, a mode of development typical of roots,
305 shoots and rhizophores in extant lycopsids (Bierhorst, 1971; Bruchmann, 1874; Gola, 2014;
306 Guttenberg, 1966; Harrison et al., 2007; Hetherington and Dolan, 2017; Imaichi, 2008;
307 Imaichi and Kato, 1989; Ogura, 1972; Øllgaard, 1979; Spencer et al., 2020; Wigglesworth,
308 1907; Yi and Kato, 2001; Yin and Meicenheimer, 2017). To investigate which mode of
309 development operated in *A. mackiei* we examined anatomy of branch points.

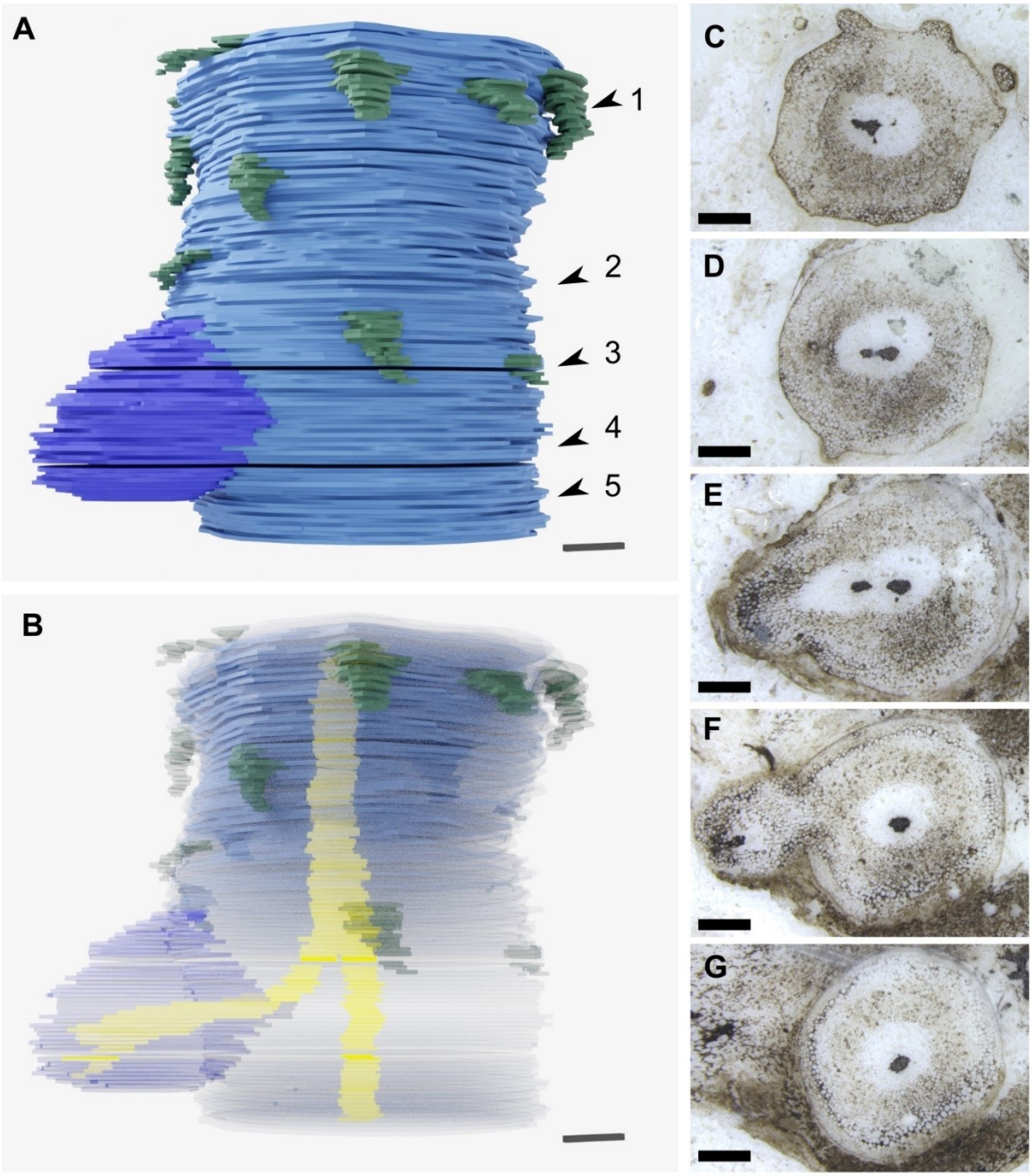

Figure 4. Rooting axes developed from root-bearing axes by dichotomous branching. A, 3D reconstruction based on 119 peels from the A. Bhutta peel collection illustrating the attachment of a rooting axis to a root-bearing axis at an anisotomous branch point. Above the branch point the root-bearing axis, in blue, is covered by small scale leaves indicated in dark green that are absent below the branch point. B, Same 3D reconstruction as in (A) but with a transparent outline of the axis so the branching of the central xylem trace can be seen in yellow. C-G, Images of representative peels used to create the 3D reconstruction showing the anatomical changes associated with branching, including the branching of the xylem strand (C, D), and the continuity of tissues between the root-bearing axis and the rooting axis (E, F). The positions of the peels (C-G) are shown with the numbered arrowheads 1-5 in (A). 3D scale bar 1 x 0.1 x 0.1 mm (A, B). Scale bars, 1 mm (C-G). A. Bhutta peel collection numbers RCA 14 (C), RCA 61 (D), RCA 81 (E), RCA 103 (F), RCA 114 (G).

If the rooting axes developed by endogenous branching from root-bearing axes there would likely be a disruption to the tissues of the leafy shoot and evidence that the vascular trace of the root-bearing axes connected at right angles to the vascular trace of the leafy shoot (Bruchmann, 1874; Guttenberg, 1966; Imaichi, 2008; Ogura, 1972; Van Tieghem and Douliot, 1888; Wigglesworth, 1907; Yi and Kato, 2001). Our thick sections only provided a small organic connection between the two axes (Figure 3C) limiting our ability to investigate the anatomical changes associated with branching. We therefore searched other Rhynie chert collections for rooting axes attached to root-bearing axes at anisotomous branching points. We reinvestigated an example originally described as a branching rhizome by Bhutta (Bhutta, 1969). The presence of scale leaves, a small number of leaf traces and clear epidermis and cuticle on the main axis suggested it was a root-bearing axis. Attached to this root-bearing axis was a smaller axis that we interpret as a rooting axis because of its rounded xylem, poorly preserved epidermis and the lack of both cuticle and root cap (Figure 4, Figure S3). We produced a 3D reconstruction of the anisotomous branch point that connects the two axes based on 119 peels (Figure 4, Movie S2). Tissues were continuous between the root-bearing axis and rooting axis. The vascular trace for the rooting axis was seen to branch off and then run parallel to the main vascular trace before gradually arcing into the rooting axis (Figure 4). These characteristics, especially the dichotomy of the vascular trace, suggest that rooting axes developed from root-bearing axes by dichotomous branching.

While branching evidence in our reconstruction is consistent with the development of rooting axes from root-bearing axes by dichotomy, we tested if there was evidence for endogenous development because roots originate endogenously in extant lycopsids (Bierhorst, 1971; Bruchmann, 1874; Fujinami et al., 2020; Guttenberg, 1966; Hetherington and Dolan, 2017; Imaichi, 2008; Imaichi and Kato, 1989; Ogura, 1972; Øllgaard, 1979; Wigglesworth, 1907; Yi and Kato, 2001). Therefore, we searched for meristems of rooting axes preserved soon after they originated from root-bearing axes. We identified two fossilised *A. mackiei* meristems on a single thin section. This thin section preserves a large *A. mackiei* leafy shoot axis ca. 5 mm in diameter with stellate xylem cut in transverse section at the top of the image (Figure 5A, green arrowhead). Attached to the leafy shoot axis is a smaller root-bearing axis ca. 1.9 mm in diameter close to the attachment with the leafy shoot. This axis is identified as a root-bearing axis by the presence of a small scale leaf (Figure 5A blue arrowhead, B), and its orientation aligned with the gravity vector based on a geopetally infilled void (Figure S1). Close to the base of the thin section are two apices on either side of the root-bearing axis (Figure 5A, white arrowheads). We interpret these as meristems because of their domed structure and the large number of small cells close to the apices. Given the attachment of

these meristems to root-bearing axes and their small size we interpret them as meristems of rooting axes. Cellular organisation of the promeristems (Figure 5C-E, Figure S4) is poorly preserved compared to other meristems we described (Hetherington and Dolan, 2018) but the overall organisation including cell files running from the central vascular trace, and a cuticle covering the apices can be clearly recognised. There is no root cap as previously reported for rooting axes (Hetherington and Dolan, 2018a). Cell files are continuous between the root-bearing axes and rooting axes and there is no evidence that the rooting axes initiated by endogenous branching and broke through the ground or dermal tissues of the root-bearing axes. The organisation of cells in these meristems is consistent with our hypothesis based on 3D reconstructed anatomy that the rooting axes developed by dichotomous branching from root-bearing axes.

We conclude that rooting axes originate by dichotomous branching of root-bearing axes in *A. mackiei*. Furthermore, the branch connecting rooting axes and root-bearing axes was always anisotomous. This finding is significant because roots do not originate by dichotomy in extant lycopsids. Instead, roots of extant lycopsids originate endogenously from shoots, rhizophores and rhizomorphs (Bruchmann, 1874; Guttenberg, 1966; Hetherington and Dolan, 2017; Imaichi, 2008; Imaichi and Kato, 1989; Ogura, 1972; Yi and Kato, 2001), and in rare cases by exogenous development not related to dichotomy of an apex, such as embryonic roots, protocorms and tubers (Bower, 1908; Hetherington and Dolan, 2017). Our findings therefore indicate that the origin of *A. mackiei* rooting axes by anisotomous dichotomy was different from the origin of roots in extant lycopsids, and this developmental mechanism is now extinct.

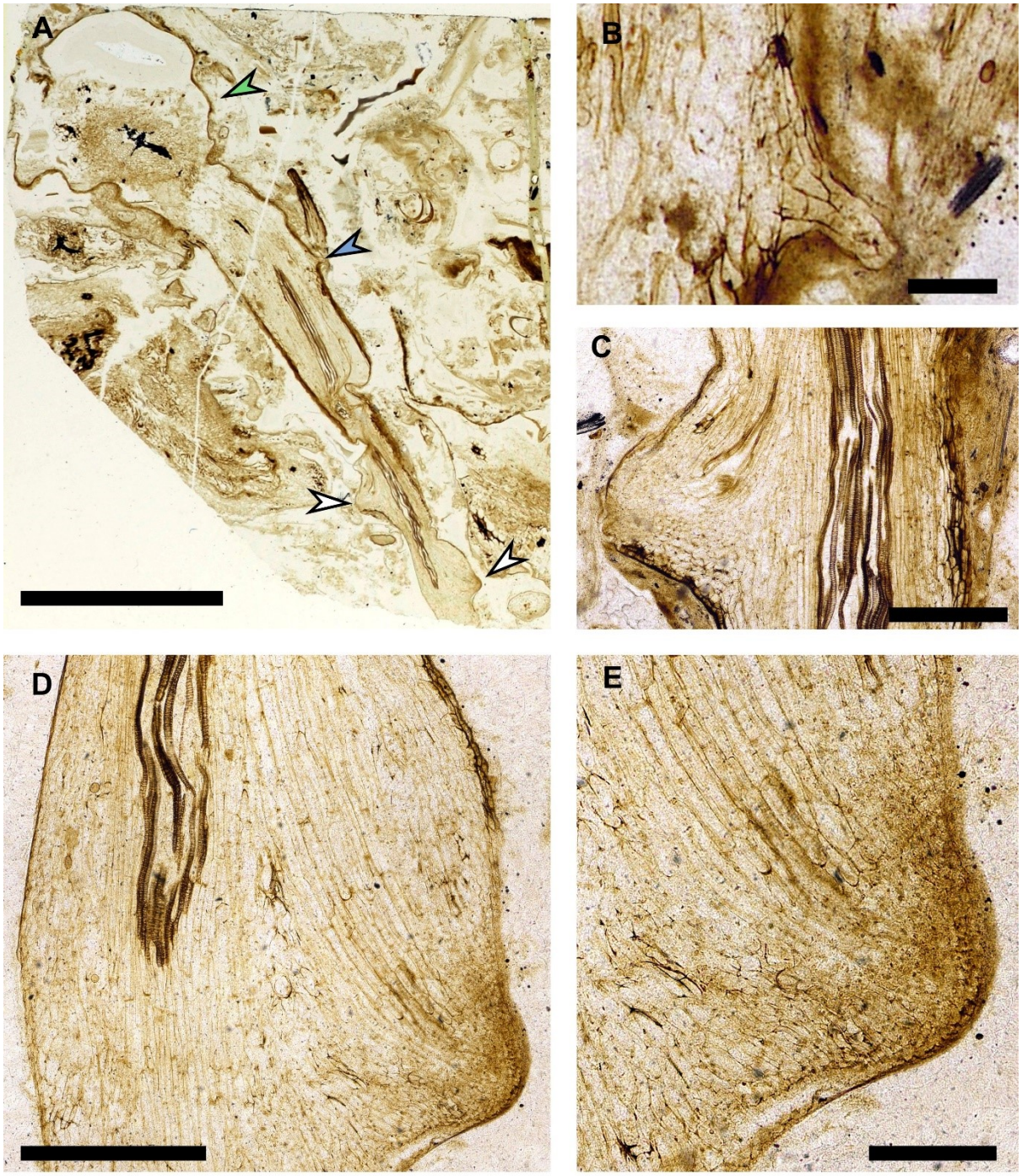

Figure 5. Fossilised meristems preserve evidence that rooting axes developed from root-bearing axes by anisotomous dichotomy. A-E, *A. mackiei* axes preserving connection between a leafy shoot axis, root-bearing axis and two rooting axes apices. A, photograph of thin section NHMUK 16433 showing a large *A. mackiei* axis with stellate xylem cut in transverse section in the top left and highlighted with the green arrowhead, and attached root-bearing axis. On the root-bearing axis (A) the position of a scale leaf (B), is highlighted with a blue arrowhead and the two rooting axes meristems are highlighted with white arrowheads. C-E, Rooting axis meristems marked by white arrowheads in (A) the left arrowhead (C) and right (D, E). D, E, Well preserved rooting axis meristem showing continuous cell files from the central vascular trace into the apex, the tissues of the rooting axis are continuous with the root-bearing axis indicating that development was by anisotomous dichotomy. Scale bars, 5 mm (A), 0.5 mm (C, D) 0.2 mm (B, E). Specimen accession codes: NHMUK 16433 (A-E).

Discussion

We draw three significant conclusions from our 3D reconstruction of *A. mackiei*. (i) The body plan of *A. mackiei* was similar to the cosmopolitan members of the Drepanophycales found across America, Europe and China in the Early and Middle Devonian (Gensel et al., 2001; Li and Edwards, 1995; Matsunaga and Tomescu, 2017, 2016; Rayner, 1984; Schweitzer, 1980; Schweitzer and Giesen, 1980; Xu et al., 2013; Xue et al., 2016). This suggests that despite inhabiting the Rhynie geothermal wetland ecosystem (Edwards et al., 2018; Garwood et al., 2020; Rice et al., 2002; Strullu-Derrien et al., 2019; Wellman, 2018), mechanisms of body plan construction in *A. mackiei* likely also operated in other Devonian Drepanophycales. (ii) We demonstrate that rooting axes originated from root-bearing axes by dichotomy. In extant lycopsids roots originate endogenously from shoots or specialised root producing organs, such as rhizophores. Once developed, roots, shoots and rhizophores branch dichotomously (Chomicki et al., 2017; Fujinami et al., 2020; Gola, 2014; Harrison et al., 2007; Hetherington and Dolan, 2017; Imaichi, 2008; Imaichi and Kato, 1991; Øllgaard, 1979; Yin and Meicenheimer, 2017). However, the two daughter axes produced by dichotomous branching are always identical to the original axis: a shoot axis may branch dichotomously to form two identical shoot axes, a root axis may branch to form two identical root axes and a rhizophore branches to form two identical rhizophores (Chomicki et al., 2017; Fujinami et al., 2020; Gola, 2014; Harrison et al., 2007; Hetherington and Dolan, 2017; Imaichi, 2008; Imaichi and Kato, 1991; Øllgaard, 1979; Yin and Meicenheimer, 2017). In *A. mackiei,* the root-bearing axes branched anisotomously to produce one root-bearing axis and a rooting axis. Our findings therefore suggest that anisotomous dichotomy was key for the development of the complex body plan of *A. mackiei*, which builds on previous suggestions that the evolution of anisotomous dichotomy in land plants was a key developmental innovation for both the evolution of leaves (Sanders et al., 2007; Stewart and Rothwell, 1993; Zimmerman, 1952) and rooting systems (Gensel et al., 2001). (iii) Finally, these findings demonstrate how 3D evidenced-based reconstructions of the Rhynie chert plants can define how these plants grew and developed. These reconstructions allow the body plans of Rhynie chert plants to be compared with plants preserved as compression fossils where body plans can be determined but cellular anatomy is not preserved.

Taken together our 3D reconstruction demonstrates that the body plan of *A. mackiei* comprised three distinct axes types and we demonstrate that roots developed through anisotomous dichotomy of a specialised root-bearing axis. This mode of rooting system development is now extinct, but played a key role in the development of the complex rooting systems of the Drepanophycales.

Materials and Methods

Specimen accession code abbreviations: Forschungsstelle für Paläobotanik, Institut für Geologie und Paläontologie, Westfälische Wilhelms-Universität, Münster, Germany; Pb. The Hunterian, University of Glasgow, GLAHM. Natural History Museum, London, NHMUK.

Thick section preparation

The reconstruction of *A. mackiei* was based on a series of 31 thick sections made from a single block of chert collected from a trench dug in 1964. Thick sections were made by mounting the rock to 2.8 cm by 4.8 cm glass slides using thermoplastic synthetic resin and cutting with a 1 mm thick diamond blade. The resulting thin wafer of rock was ground with silicon carbide powder to ensure a flat surface, a number of specimens were released from the glass slide and turned around to grind them down further from the other side (Hass and Rowe, 1999). Thick sections were not sealed with a cover slip and were deposited in the collection of the Forschungsstelle für Geologie und Paläontologie, Westfälische Wilhelms-Universität, Münster, Germany under the accession numbers Pb 4161-4191.

3D reconstruction of *A. mackiei* from thick sections

To create a 3D reconstruction based on the series of thick sections, photographs of the upper and lower surface of the thick sections were taken. Thick sections were placed on a milk glass pane above a lightbox and incident light was provided by two lamps (Kerp and Bomfleur, 2011). The surface of the specimen was covered with cedar wood oil and images were captured with a Canon MP-E 65 mm macro lens and a Canon EOS 5D Mark IV single-lens reflex camera. Images of the full series of thick sections were deposited on Zenodo (http://doi.org/10.5281/zenodo.4287297). Line drawings were made of both the outline of the *A. mackiei* axes of interest and also the central vascular trace in each axis using Inkscape (https://inkscape.org/). Line drawings were imported into Blender (https://www.blender.org/) and extruded in the z-dimension by 0.2 mm to turn each outline into a 3D slice. In the model, a thick section was then represented by an upper and lower slice of 0.2 mm separated by a gap of 0.4 mm. Slices from consecutive thick sections were aligned and a 1 mm gap was left to represent the material lost to the saw blade when making the sections. Images and animations of the reconstruction were made in Blender, and the 3D reconstruction was deposited on Zenodo (http://doi.org/10.5281/zenodo.4287297).

3D reconstruction of *A. mackiei* from peels

A branching root-bearing axis was reconstructed from a series of RCA 1–119 from the A. Bhutta collection (Bhutta, 1969) at the University of Cardiff. Four peels were missing from the series, RCA 3, RCA 31, RCA 80 and RCA 102. Images of peels were scanned using an Epson perfection V500. Images of the full series of peels were deposited on Zenodo (http://doi.org/10.5281/zenodo.4287297). Line drawings were made of the outline of the *A. mackiei* axis of interest and also the central vascular trace in each axis using Inkscape (https://inkscape.org/). Line drawings were imported into blender and extruded in the z-dimension by 0.058 mm based on (Bhutta, 1969). Consecutive slices were aligned to produce the 3D model, and gaps were left for the four missing peels. The 3D reconstruction was deposited on Zenodo (http://doi.org/10.5281/zenodo.4287297).

Higher magnification images and microscopy

Thick sections were placed on a milk glass pane above a lightbox and incident light was provided by two lamps and the surface covered in cedar wood oil (Kerp and Bomfleur, 2011). Photographs were taken with a Canon EOS 5D Mark IV digital single-lens reflex camera mounted on a copy stand using either a Canon MP-E 65 mm or Canon EFS 60 mm macro lens (Figure 1H-J, Figure 2B, C, G-K, Figure 3B-D, F, Figure S1A, B, Figure S2A-D). The photograph of thin section NHMUK 16433 (Figure 5C, Figure S1C) was taken with a Nikon D80 camera with a 60-mm macro lens mounted on a copystand with light from below from a lightbox. Higher magnification images were taken of the branching *A. mackiei* axis from the A. Bhutta collection with a Leica M165 FC with light from above provided by a Leica LED ring illuminator. (Figure 4C-G, Figure S3). Microscope images of NHMUK 16433 (Figure 5D-G, Figure S4) were taken with a Nikon Eclipse LV100ND.

Data availability Statement

Fossil preparations described in this study are housed in the A. Bhutta collection at the University of Cardiff, UK. Forschungsstelle für Paläobotanik, Institut für Geologie und Paläontologie, Westfälische Wilhelms-Universität, Münster, Germany. The Hunterian, University of Glasgow, UK and the Natural History Museum, London, UK.

Photographs of the series of thick sections and peels used to create 3D reconstructions of *A. mackie* have been deposited on Zenodo (http://doi.org/10.5281/zenodo.4287297). All other

498 data supporting the findings of this study are included in the paper and its Extended Data
499 and Supplementary Information.

500

501 **Acknowledgements**

502 A.J.H. was funded by the George Grosvenor Freeman Fellowship by Examination in
503 Sciences, Magdalen College (University of Oxford), a grant from the Hester Cordelia
504 Parsons Fund University of Oxford and a UK Research and Innovation Future Leaders
505 Fellowship MR/T018585/1. A.L.J. was funded by a BBSRC Research Experience
506 Placement, Oxford cohort 2019. L.D. by a European Research Council Advanced Grant
507 (EVO500, contract 250284), and European Research Council Grant (De NOVO-P, contract
508 787613). L.D. and H.K. were supported by European Commission Framework 7 Initial
509 Training Network (PLANTORIGINS, contract 238640). H.K. and H.H. were funded by the
510 German Science Foundation (DFG Grant KE 584/13- 1 and 2). We would like to thank D.
511 Edwards for access to the Bhutta collection at the University of Cardiff, P. Hayes for access
512 to collection at the NMHUK and J. Hetherington for drawing Figure 1G.

513

514 **Author contributions**,

515 A.J.H. designed the project with advice from L.D.. H.K. and H.H. prepared fossil thick
516 sections and A.J.H., and H.K. photographed fossil thick sections. A.J.H., S.B. and A.L.J.
517 constructed the 3D reconstructions of *A. mackiei*. A.J.H. and L.D. wrote the paper with
518 comments from other co-authors.

519

520 **Competing Interest Statement:** The authors declare no competing interests.

521

522

523 **References**

524 Algeo TJ, Scheckler SE. 1998. Terrestrial-marine teleconnections in the Devonian: links
525 between the evolution of land plants, weathering processes, and marine anoxic events.
526 *Philos Trans R Soc B Biol Sci* **353**:113–130. doi:10.1098/rstb.1998.0195

527 Bateman RM, Crane PR, DiMichele WA, Kenrick PR, Rowe NP, Speck T, Stein WE. 1998.
528 Early evolution of land plants: phylogeny, physiology and ecology of the primary

terrestrial radiation. *Annu Rev Ecol Syst* **29**:263–292. doi:10.1146/annurev.ecolsys.29.1.263

Bhutta AA. 1969. Studies on the flora of the Rhynie Chert. PhD thesis. University of Wales, Cardiff (UK).

Bierhorst DW. 1971. Morphology of vascular plants. New York (USA): Macmillan.

Bower FO. 1908. The origin of a land flora. London (UK): Macmillan and Co., Limited.

Bruchmann H. 1874. Ueber Anlage und Wachsthum der Wurzeln von *Lycopodium* und *Isoetes*. Jenaische Zeitschrift. Für. Naturwissenschaft. pp. 522–578.

Chaloner WG, MacDonald P. 1980. Plants invade the land. Edinburgh: H.M.S.O. for the Royal Scottish Museum.

Chomicki G, Coiro M, Renner SS. 2017. Evolution and ecology of plant architecture: integrating insights from the fossil record, extant morphology, developmental genetics and phylogenies. *Ann Bot* **120**:855–891. doi:10.1093/aob/mcx113

Edwards D. 2004. Embryophytic sporophytes in the Rhynie and Windyfield cherts. *Trans R Soc Edinburgh, Earth Sci* **94**:397–410. doi:10.1017/s0263593300000778

Edwards D. 1994. Towards an understanding of pattern and process in the growth of early vascular plants. In: Ingram D, Hudson A, editors. Shape and Form in Plants and Fungi, Linnean Society Symposium Series, Vol. 16. London: Linnean Society of London (Academic Press). pp. 39–59.

Edwards D, Kenrick P, Dolan L. 2018. History and contemporary significance of the Rhynie cherts—our earliest preserved terrestrial ecosystem. *Philos Trans R Soc B Biol Sci* **373**:20160489. doi:10.1098/rstb.2016.0489

Fujinami R, Nakajima A, Imaichi R, Yamada T. 2020. *Lycopodium* root meristem dynamics supports homology between shoots and roots in lycophytes. *New Phytol* **229**: 460-468. doi:10.1111/nph.16814

Garwood RJ, Oliver H, Spencer ART. 2020. An introduction to the Rhynie chert. *Geol Mag* **157**:47–64. doi:10.1017/S0016756819000670

Gensel PG, Berry CM. 2001. Early lycophyte evolution. *Am Fern J* **91**:74–98. doi:10.1640/0002-8444(2001)091[0074:ELE]2.0.CO;2

Gensel PG, Edwards D. 2001. Plants invade the land : evolutionary and environmental perspectives. New York (USA): Columbia University Press.

560 Gensel PG, Kotyk ME, Brasinger JF. 2001. Morphology of above- and below-ground
561 structures in Early Devonian (Pragian–Emsian) plants In: Gensel PG, Edwards D,
562 editors. Plants Invade the Land: Evolutionary and Environmental Perspectives. New
563 York (USA): Columbia University Press. pp. 83–102.

564 Gerrienne P. 1988. Early Devonian plant remains from Marchin (North of Dinant
565 Synclinorium, Belgium), I. *Zosterophyllum deciduum* sp. nov. *Rev Palaeobot Palynol*
566 **55**:317–335. doi:10.1016/0034-6667(88)90091-7

567 Gibling MR, Davies NS. 2012. Palaeozoic landscapes shaped by plant evolution. *Nat Geosci*
568 **5**:99–105. doi:10.1038/ngeo1376

569 Gola EM. 2014. Dichotomous branching: the plant form and integrity upon the apical
570 meristem bifurcation. *Front Plant Sci* **5**:1–7. doi:10.3389/fpls.2014.00263

571 Guttenberg HV. 1966. Histogenese der Pteridophyten. Handbuch der Pflanzenanatomie vol.
572 VII. 2. Berlin, Germany: Gebrüder Borntraeger.

573 Harrison CJ, Rezvani M, Langdale JA. 2007. Growth from two transient apical initials in the
574 meristem of *Selaginella kraussiana*. *Development* **134**:881–889.
575 doi:10.1242/dev.001008

576 Hass H, Rowe NP. 1999. Thin sections and wafering In: Jones TP, Rowe NP, editors. Fossil
577 Plants and Spores: Modern Techniques. Geological Society, London. pp. 76–81.

578 Hetherington AJ, Dolan L. 2019. Rhynie chert fossils demonstrate the independent origin
579 and gradual evolution of lycophyte roots. *Curr Opin Plant Biol* **47**:119–126.
580 doi:10.1016/j.pbi.2018.12.001

581 Hetherington AJ, Dolan L. 2018a. Stepwise and independent origins of roots among land
582 plants. *Nature* **561**:235–238. doi:10.1038/s41586-018-0445-z

583 Hetherington AJ, Dolan L. 2018b. Bilaterally symmetric axes with rhizoids composed the
584 rooting structure of the common ancestor of vascular plants. *Philos Trans R Soc B Biol*
585 *Sci* **373**:20170042. doi:10.1098/rstb.2017.0042

586 Hetherington AJ, Dolan L. 2017. The evolution of lycopsid rooting structures: conservatism
587 and disparity. *New Phytol* **215**:538–544. doi:10.1111/nph.14324

588 Hueber FM. 1992. Thoughts on the early Lycopsids and Zosterophylls. *Ann Missouri Bot*
589 *Gard* **79**:474–499.

590 Imaichi R. 2008. Meristem organization and organ diversity In: Ranker TA, Haufler CH,
591 editors. Biology and Evolution of Ferns and Lycophytes. Cambridge: Cambridge

University Press. pp. 75–104. doi:10.1017/CBO9780511541827.004

Imaichi R, Kato M. 1991. Developmental study of branched rhizophores in three *Selaginella* species. *Am J Bot* **78**:1694–1703. doi:10.2307/2444848

Imaichi R, Kato M. 1989. Developmental anatomy of the shoot apical cell, rhizophore and root of *Selaginella uncinata*. *Bot Mag Tokyo* **102**:369–380. doi:10.1007/BF02488120

Kenrick P. 2002. The telome theory In: Cronk QCB, Bateman RM, Hawkins J, editors. Developmental Genetics and Plant Evolution. London: Taylor & Francis. pp. 365–387.

Kenrick P, Crane PR. 1997. The origin and early diversification of land plants: a cladistic study. Smithsonian Series in Comparative Evolutionary Biology. Washington, DC, USA: Smithsonian Institute Press.

Kerp H. 2018. Organs and tissues of Rhynie chert plants. *Philos Trans R Soc B Biol Sci* **373**:20160495. doi:10.1098/rstb.2016.0495

Kerp H, Bomfleur B. 2011. Photography of plant fossils—New techniques, old tricks. *Rev Palaeobot Palynol* **166**:117–151. doi:10.1016/j.revpalbo.2011.05.001

Kerp H, Wellman CH, Krings M, Kearney P, Hass H. 2013. Reproductive organs and in situ spores of *Asteroxylon mackiei* Kidston & Lang, the most complex plant from the Lower Devonian Rhynie Chert. *Int J Plant Sci* **174**:293–308. doi:10.1086/668613

Kidston R, Lang WH. 1920. On Old Red Sandstone plants showing structure, from the Rhynie Chert Bed, Aberdeenshire. Part III. *Asteroxylon mackiei*, Kidston and Lang. *Trans R Soc Edinb Earth Sci* **52**:643–680.

Kidston R, Lang WH. 1921. On Old Red Sandstone plants showing structure, from the Rhynie Chert Bed, Aberdeenshire. Part IV. Restorations of the vascular cryptogams, and discussion of their bearing on the general morphology of the Pteridophyta and the origin of the organisation of land plants *Trans R Soc Edinb Earth Sci* **52**:831–854.

Lang WH, Cookson IC. 1935. On a flora, including vascular land plants, associated with *Monograptus*, in rocks of Silurian age, from Victoria, Australia. *Philos Trans R Soc Lond B Biol Sci* **224**:421–449. doi:10.1098/rstb.1935.0004

Li CS, Edwards D. 1995. A reinvestigation of Halle's D*repanophycus spinaeformis* Göpp. from the Lower Devonian of Yunnan Province, Southern China. *Bot J Linn Soc* **118**:163–192.

Lyon AG. 1964. Probable fertile region of *Asteroxylon mackiei* K. and L. *Nature* **203**:1082–1083. doi:10.1038/2031082b0

624 Lyon AG. 1957. Germinating spores in the Rhynie Chert. *Nature* **180**:1219–1219.
625 doi:10.1038/1801219a0

626 Matsunaga KKS, Tomescu AMF. 2016. Root evolution at the base of the lycophyte clade:
627 insights from an Early Devonian lycophyte. *Ann Bot* **117**:585–598.
628 doi:10.1093/aob/mcw006

629 Matsunaga KKS, Tomescu AMF. 2017. An organismal concept for *Sengelia radicans* gen. et
630 sp. nov. – morphology and natural history of an Early Devonian lycophyte. *Ann Bot*
631 **119**:1097–1113. doi:10.1093/aob/mcw277

632 Ogura Y. 1972. Comparative anatomy of vegetative organs of the pteridophytes. Handb
633 Pflanzenanat, Second. ed. Berlin, Germany: Gebrüder Borntraeger.

634 Øllgaard B. 1979. Studies in Lycopodiaceae, II. The branching patterns and infrageneric
635 groups of *Lycopodium* sensu lato. *Am Fern J* **69**:49. doi:10.2307/1546896

636 Rayner RJ. 1984. New finds of *Drepanophycus spinaeformis* Göppert from the Lower
637 Devonian of Scotland. *Trans R Soc Edinb Earth Sci* **75**:353–363.

638 Rice CM, Trewin NH, Anderson LI. 2002. Geological setting of the Early Devonian Rhynie
639 cherts, Aberdeenshire, Scotland: an early terrestrial hot spring system. *J Geol Soc*
640 *London* **159**:203–214. doi:10.1144/0016-764900-181

641 Sanders H, Rothwell GW, Wyatt S. 2007. Paleontological context for the developmental
642 mechanisms of evolution. *Int J Plant Sci* **168**:719–728. doi:10.1086/513519

643 Schweitzer H-J. 1980. Über *Drepanophycus spinaeformis* Göppert. *Bonner Paläobotanische*
644 *Mitteilungen* **7**:1–29.

645 Schweitzer H-J, Giesen P. 1980. Über *Taeniophyton inopinatum*, *Protolycopodites*
646 *devonicus* und *Cladoxylon scoparium* aus dem Mitteldevon von Wuppertal. *Palaeontogr*
647 *Abteilung B* **173**:1–25.

648 Spencer V, Nemec Venza Z, Harrison CJ. 2020. What can lycophytes teach us about plant
649 evolution and development? Modern perspectives on an ancient lineage. *Evol Dev*
650 **e12350**. doi:10.1111/ede.12350

651 Stewart W, Rothwell GW. 1993. Paleobotany and the evolution of plants, Second. ed.
652 Cambridge (UK): Cambridge University Press.

653 Strullu-Derrien C, Kenrick P, Knoll AH. 2019. The Rhynie chert. *Curr Biol* **29**:R1218–R1223.
654 doi:10.1016/j.cub.2019.10.030

655 Taylor TN, Kerp H, Hass H. 2005. Life history biology of early land plants: deciphering the
656 gametophyte phase. *Proc Natl Acad Sci U S A* **102**:5892–5897.
657 doi:10.1073/pnas.0501985102

658 Van Tieghem P, Douliot H. 1888. Recherches comparatives sur l'origine des membres
659 endogenes dans les plantes vasculaires. *Ann des Sci Nat Bot Paris* **8**:1–656.

660 Wellman CH. 2018. Palaeoecology and palaeophytogeography of the Rhynie chert plants:
661 further evidence from integrated analysis of in situ and dispersed spores. *Philos Trans*
662 *R Soc B Biol Sci* **373**:20160491. doi:10.1098/rstb.2016.0491

663 Wigglesworth G. 1907. The young sporophytes of *Lycopodium complanatum* and
664 *Lycopodium clavatum*. *Ann Bot* **21**:211–234.

665 Xu H-H, Feng J, Jiang Q, Wang Y. 2013. Report of *Drepanophycus* Göppert (Lycopsida)
666 from the Middle Devonian of Xinjiang, China. *J Syst Evol* **51**:765–772.
667 doi:10.1111/jse.12043

668 Xue J, Deng Z, Huang P, Huang K, Benton MJ, Cui Y, Wang D, Liu J, Shen B, Basinger JF,
669 Hao S. 2016. Belowground rhizomes in paleosols: The hidden half of an Early
670 Devonian vascular plant. *Proc Natl Acad Sci* **113**:9451–9456.
671 doi:10.1073/pnas.1605051113

672 Xue J, Huang P, Wang D, Xiong C, Liu L, Basinger JF. 2018. Silurian-Devonian terrestrial
673 revolution in South China: Taxonomy, diversity, and character evolution of vascular
674 plants in a paleogeographically isolated, low-latitude region. *Earth-Science Rev*
675 **180**:92–125. doi:10.1016/j.earscirev.2018.03.004

676 Yi S, Kato M. 2001. Basal meristem and root development in *Isoetes asiatica* and *Isoetes*
677 *japonica*. *Int J Plant Sci* **162**:1225–1235.

678 Yin X, Meicenheimer RD. 2017. Anisotomous dichotomy results from an unequal bifurcation
679 of the original shoot apical meristem in *Diphasiastrum digitatum* (Lycopodiaceae). *Am J*
680 *Bot* **104**:782–786. doi:10.3732/ajb.1700021

681 Zimmerman W. 1952. Main results of the "Telome Theory." *Palaeobot* **1**:456–470.

682

683

684

685

686 **Supplementary figures**

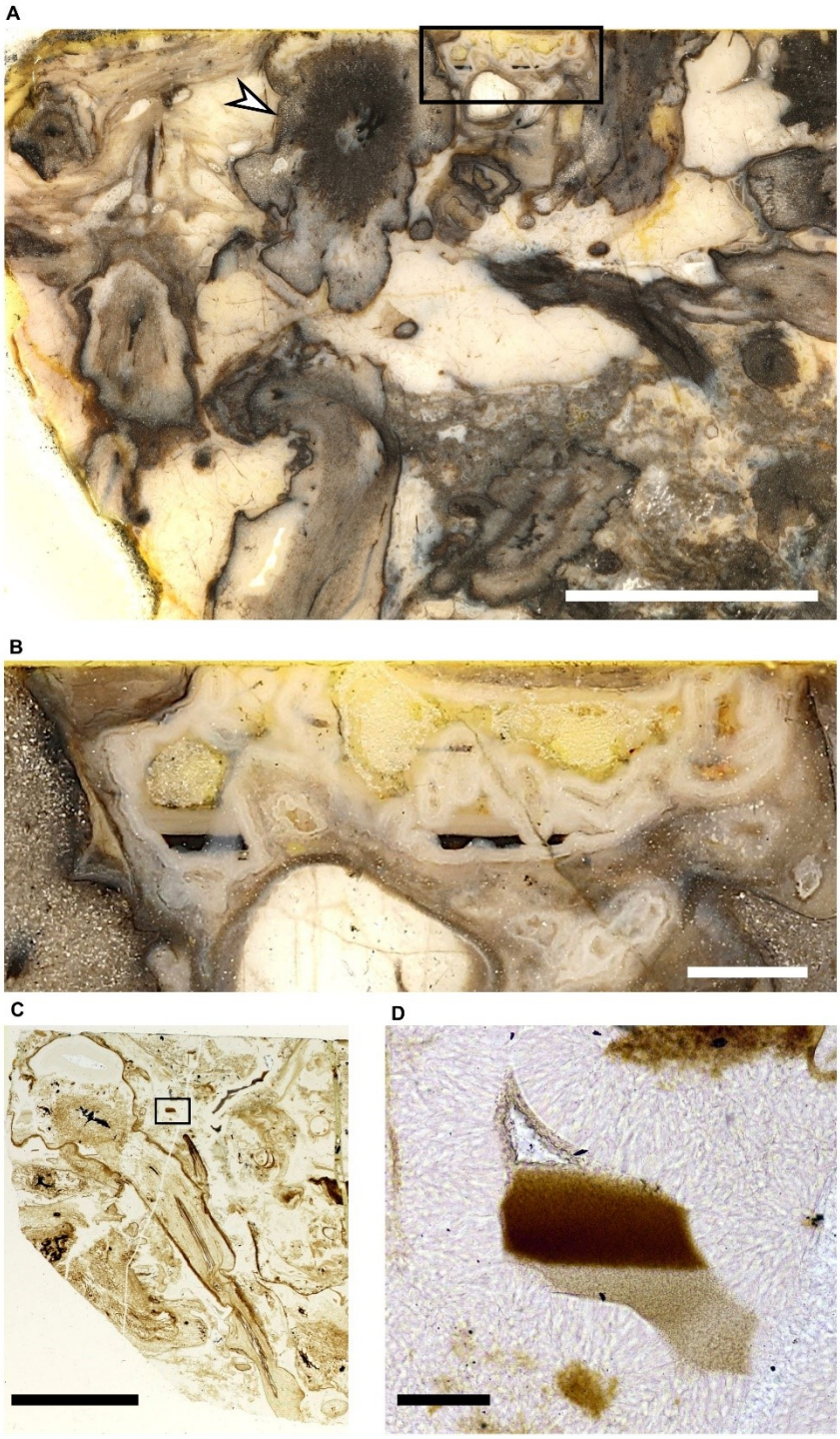

687
688 **Figure S1.** Geopetally infilled voids allow growth orientation to be established. A, B, A
689 geopetally infilled void highlighted in the black box in (A) and magnified in (B) enabled the
690 establishment of the growth orientation for the main *A. mackiei* leafy shoot axis present in all
691 thick sections in the series, indicated with the white arrowhead. C, D, A geopetally infilled
692 void highlighted in the black box in (C) and magnified in (D) enabled us to establish the
693 growth orientation of the shoot-borne rooting axis described in Figure 5. Scale bars, 1 cm
694 (A), 5 mm (C), 1 mm (B), 200 µm (D). Specimen accession codes: Pb 4161 (A, B), NHMUK
695 16433 (C, D).

696

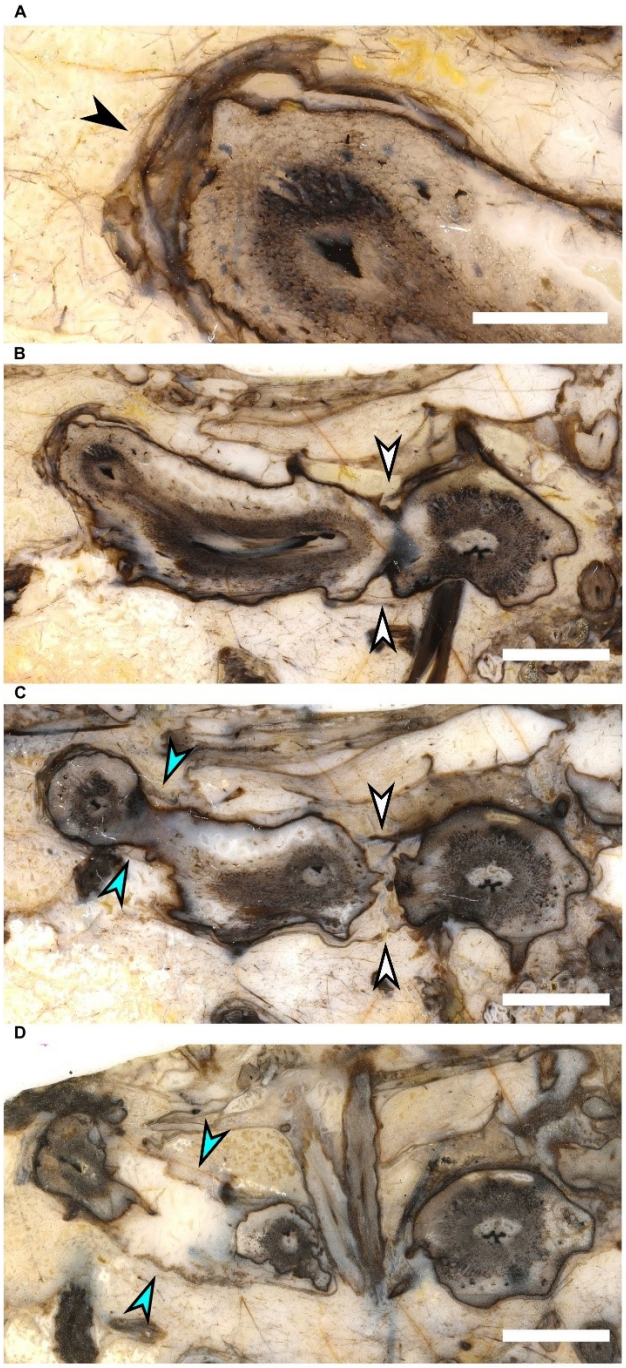

Figure S2. *A. mackiei* axes were preserved in original growth position. The peaty substrate the *A. mackiei* axes were growing through consisted of plant material in various states of decay and organic films. These organic films were often found covering the outside of axes such as the layer highlighted with the black arrowhead (A). B-D, At branch points the organic film was stretched round the two daughter axes. White and blue arrowheads (B, C) highlight examples of this stretching across both the upper and lower surface of two consecutive branching events. The way the organic film was stretched and the substrate deformed by the branching of the *A. mackiei* axes suggests these axes were preserved *in situ*. Scale bars, 0.2 cm (A), 0.5 mm (B-D). Specimen accession codes: Pb 4171 (A, B), Pb 4172 (C), Pb 4173 (D).

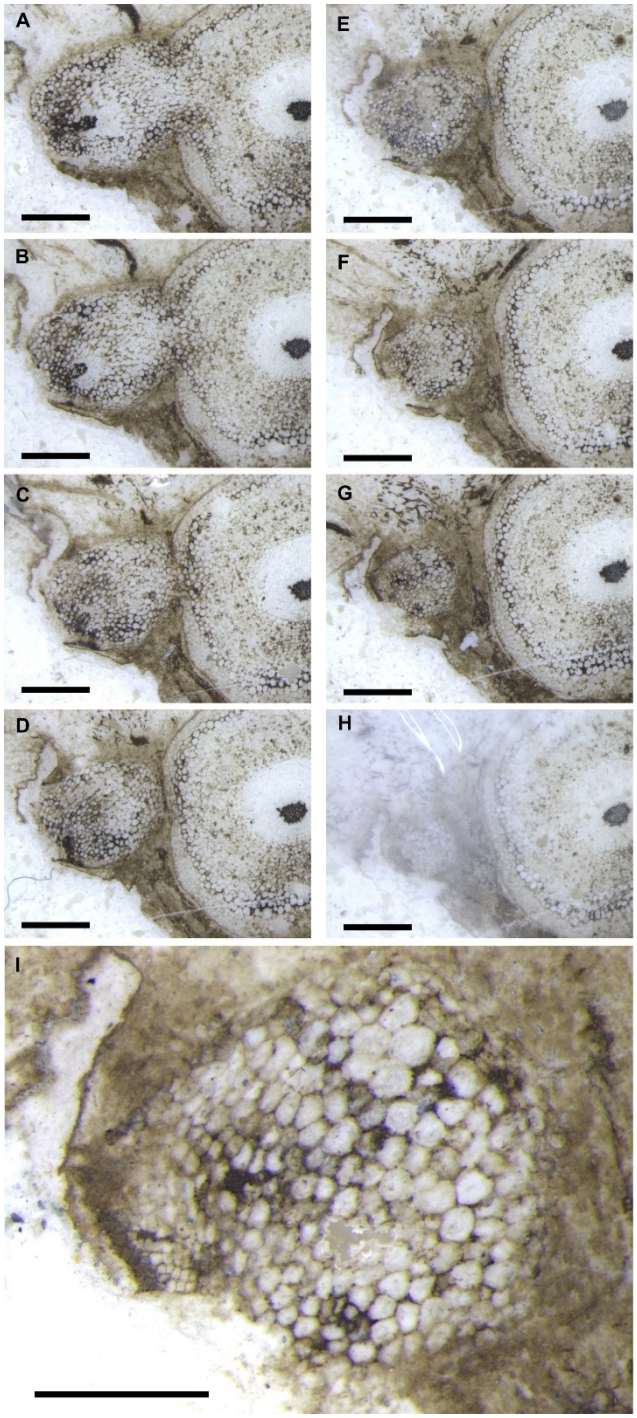

Figure S3. Rooting axes lacked cuticles and root caps. A-H, Serial peels through the apex of a rooting axis described in text Figure 4C-G. The axis gradually decreases in size towards the apex and there is no evidence of a cuticle, root cap or cap like covering of the apex including the presence of large cells outside of the epidermis and a surrounding ring of cells sloughed off into the substrate. I, Higher magnification image of (G), the last well preserved specimen of the rooting axis. Specimen accession codes: Bhutta peel collection numbers RCA 103 (A), RCA 104 (B), RCA 106 (C), RCA 107 (D), RCA 108 (E), RCA 109 (F), RCA 110 (G, I), RCA 112 (H). Scale bars, 1 mm (A-H), 500 μm (I).

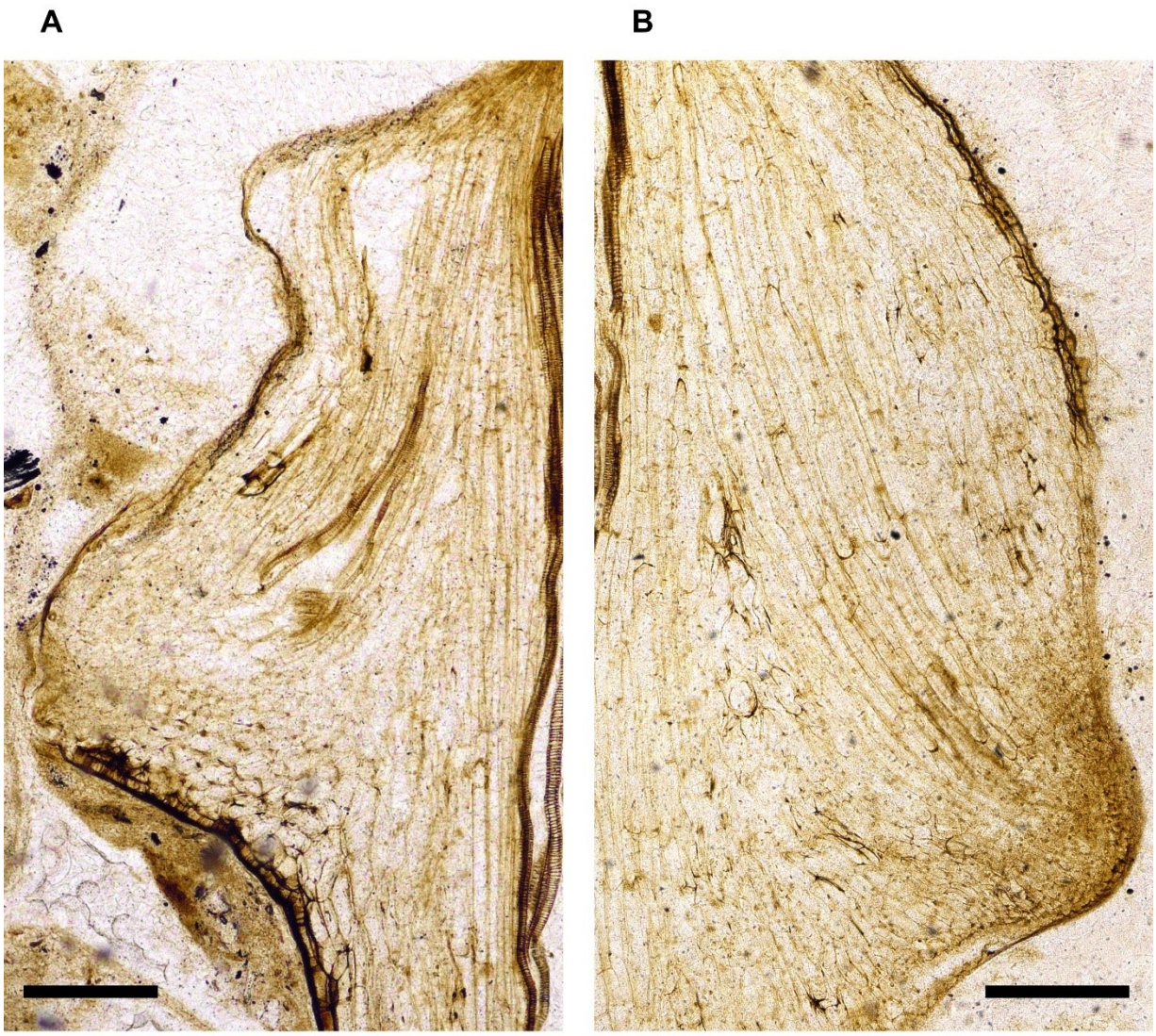

Figure S4. *A. mackiei* fossilised rooting axes meristems. A, B Enlarged image of the two fossilised *A. mackiei* rooting axes meristems shown in text Figure 5. A, B, Enlarged images of Figure 5C, D showing details of the rooting axis meristems including the cell files leading into the apices from the central vascular trace and the lack of a root cap covering the apices. Scale bars, 250 μm (A, B). Specimen accession codes: NHMUK 16433 (A, B).

Movie S1 (separate file). 3D reconstruction of *A. mackiei* based on serial thick sections. A 3D reconstruction based on a series of 31 thick sections deposited in the collection of the Forschungsstelle für Geologie und Paläontologie, Westfälische Wilhelms-Universität, Münster, Germany under the accession numbers Pb 4161-4191. Leafy shoot axes in green, root-bearing axes in blue and rooting axes in purple. 3D scale bar 1 x 0.1 x 0.1 cm.

Movie S2 (separate file). 3D reconstruction of *A. mackiei* based on serial peels. A 3D reconstruction based on 119 peels from the A. Bhutta peel collection, University of Cardiff, illustrating the attachment of a rooting axis (purple) to a root-bearing axis (blue) at an anisotomous branch point. Small scale leaves on the root-bearing axis indicated in dark green 3D scale bar 1 x 0.1 x 0.1 mm.